Could a Decentralized Onsite Earthquake Early Warning System Help in Mitigating Seismic Risk in Northeastern Italy? The Case of the 1976 M_s 6.5 Friuli Earthquake

Stefano Parolai[1], Luca Moratto[2], Michele Bertoni[2], Chiara Scaini*[2], and Alessandro Rebez[1]

Abstract

In May 1976, a devastating earthquake of magnitude M_s 6.5 occurred in Friuli, Italy, resulting in 976 deaths, 2000 injured, and 60,000 homeless. It is notable that, at the time of the earthquake, only one station was installed in the affected region. The resulting lack of information, combined with a dearth of mitigation planning for responding to such events, lead to a clear picture of the impact of the disaster being available only after a few days.

This region is now covered by nearly 100 seismological and strong-motion stations operating in real time. Furthermore, 30 average-cost strong-motion stations have been recently added, with the goals of improving the density of real-time ground-motion observations and measuring the level of shaking recorded at selected buildings. The final goal is to allow rapid impact estimations to be made to improve the response of civil protection authorities. Today, considering the higher density seismological network, new efforts in terms of the implementation and testing of earthquake early warning systems as a possible tool for mitigating seismic risk are certainly worthwhile.

In this article, we show the results obtained by analyzing in playback and using an algorithm for decentralized onsite earthquake early warning, broadband synthetic strong-motion data calculated at 18 of the stations installed in the region, while considering the magnitude and location of the 1976 Friuli earthquake. The analysis shows that the anisotropy of the lead times is related not only to the finite nature of the source but also to the slip distribution. A reduction of 10% of injured persons appears to be possible if appropriate mitigating actions are employed, such as the development of efficient automatic procedures that improve the safety of strategic industrial facilities.

Introduction

The Friuli area (northeastern Italy), due to the south-verging fold-and-thrust belt of the eastern–southern Alps joining the northwest–southeast-trending dextral strike-slip fault system of western Slovenia, is affected by moderate to strong earthquakes, mainly with thrust mechanisms. The Parametric Catalogue of Italian Earthquakes 15 (Rovida *et al.*, 2016) reports that between 1000 and 1975, six events of M_w greater than 6 occurred in the region.

In May 1976, a devastating earthquake of magnitude M_s 6.5 occurred in Friuli, Italy, near the town of Gemona, resulting in 976 deaths, 2000 injured, and 60,000 homeless (Zamberletti, 2018). Because of two further shocks that occurred in September 1976, 40,000 people were displaced to the Adriatic coast, far away from the epicentral area (Zamberletti, 2018). It is notable that at the time of the earthquake, only 33 seismological stations were operating within the entire Italian territory, and only one was located in the affected region (the Trieste World-Wide Standardized Seismograph Network TRI station, located nearly 70 km from the epicenter; Rebez *et al.*, 2018; Slejko, 2018). This lack of information, combined with a dearth of mitigation planning for responding to such events, led to a clear picture of the impact of the disaster only being available after a few days.

As a result of this event, it was decided that the region needed to be covered by a seismological network that could guarantee seismic monitoring. This has led to the region now being

1. National Institute of Oceanography and Applied Geophysics – OGS, Sgonico, Italy;
2. National Institute of Oceanography and Applied Geophysics – OGS, Udine, Italy
*Corresponding author: cscaini@inogs.it

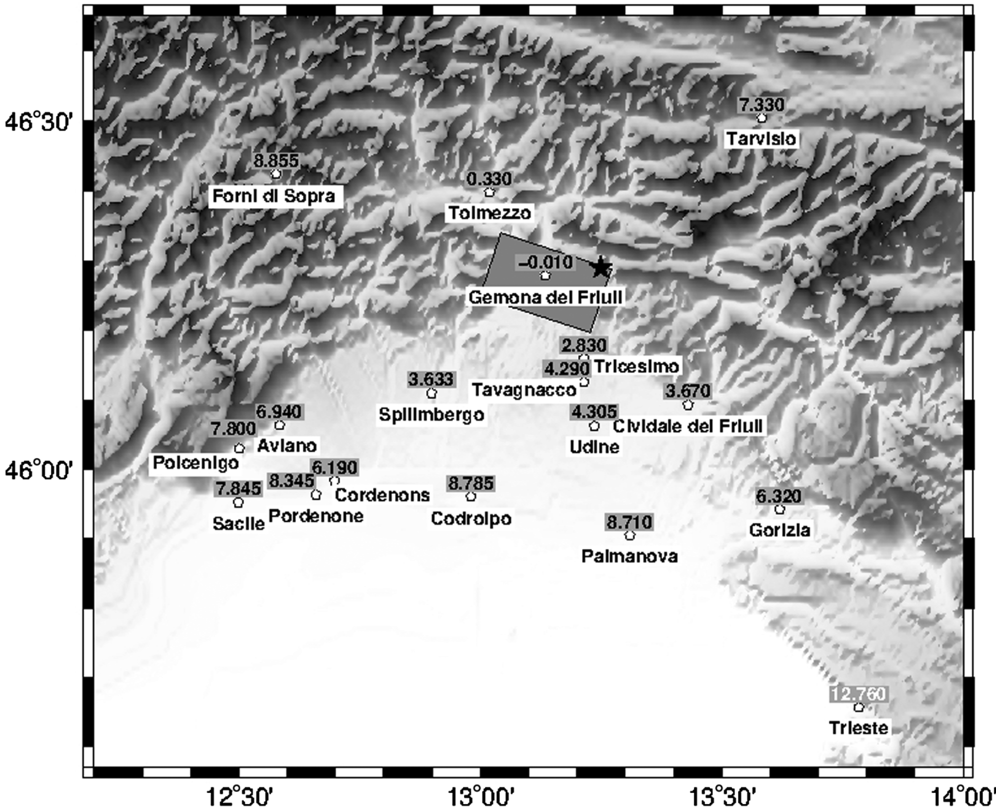

Figure 1. Locations of the strong-motion stations used for the synthetic seismogram calculations in this study (circles). The gray rectangle indicates the surface projection of the finite fault used in the calculations. The star indicates the epicenter position. The lead time (in seconds) calculated in the employed procedure for each station are depicted: black numbers indicates a red alarm and white numbers a green alarm.

covered by nearly 100 seismological and strong-motion stations operating in real time to which, recently, within the framework of two projects (Progetto Edifici Sentinella, supported by the Regional Civil Protection of Friuli Venezia Giulia, and the Interreg Armonia Project, see Data and Resources), several new real-time strong-motion stations have been added. These new stations consist of lower-cost instruments; hence they can be installed widely across the region, with the goals of improving the density of ground-motion observations and measuring the level of shaking recorded at selected buildings (referred to in the following as Sentinella buildings). The final goal is to allow rapid impact estimations to be made to improve the response of civil protection authorities.

Picozzi *et al.* (2015) and Pesaresi *et al.* (2017) already tested the possibility of implementing a regional early warning system using the Probabilistic and Evolutionary early warning SysTem (PRESTo) platform to support civil protection authorities with the rapid provision of robust forecasts and information about the earthquake-induced shaking.

Today, considering the higher density seismological network, new efforts in terms of the implementation and testing of earthquake early warning (EEW) systems (e.g., Wenzel and Zschau, 2014; Clinton *et al.*, 2016; Strauss and Allen, 2016; Wu *et al.*, 2016) as a possible tool for mitigating seismic risk are certainly worthwhile. In particular, the suitability of an onsite earthquake early warning (OSEEW) (Allen *et al.*, 2009) and specifically of a decentralized OSEEW (DOSEEW; i.e., leaving all of the analysis and actions to be carried out directly on the sensor), should be explored as an alternative or complement to the already investigated regional approach.

In this study, we simulate broadband synthetic strong-motion data at 18 of the stations installed as part of the Edifici Sentinella project for the case of the 1976 Friuli earthquake. The synthetic seismograms are analyzed in playback, reproducing a real-time analysis using the algorithm developed by Parolai *et al.* (2015) and tested by Parolai, Oth, and Boxberger (2017) for OSEEW. The obtained results were used to investigate whether the application of the OSEEW system, which can also be used in a decentralized way, might have been useful in mitigating the impact of the Friuli event and if it would be of use today in the event of its repetition. The analyses provide interesting results on the influence of both the finite nature of the source and the slip distribution (effects that very often are neglected in standard EEW approaches) on the available lead time. Moreover, efforts are made to quantify the mitigation value of an EEW system, both for the general population and for existing strategic industrial infrastructures.

Broadband Simulations for the 1976 Friuli Earthquake

The OSEEW algorithm was tested using waveforms calculated to reproduce the shaking generated by the 1976 Friuli earthquake. The broadband seismograms are computed for 18 receivers' locations, representing selected stations installed at the "Sentinella" buildings (Fig. 1) by means of the hybrid approach developed by Moratto *et al.* (2015). Within this approach, the wavefields computed by a deterministic calculation ($f < 1$ Hz) are merged with those computed by a stochastic procedure ($f > 1$ Hz). A discrete wavenumber technique, COMPSYN (Spudich and Xu, 2003), is used for the deterministic computation, and the EXSIM approach (Motazedian and Atkinson, 2005; Boore, 2009) is used for the stochastic calculations.

The input parameters for the deterministic calculations are the finite-fault parameters, the propagation model, and, if available, soil amplification functions. In this study, the source parameters are taken from Aoudia *et al.* (2000), who proposed a finite-fault rupturing model after a joint interpretation of event location seismic-wave inversion results, and field geology. In their study, the hypocenter (Fig. 1) was located at a depth of 7 km and the moment magnitude was estimated as 6.47. The focal mechanism is a thrust with a rupture extent 18.5 km long and 11.2 km wide with a unilateral rupture propagating toward west–northwest (Fig. 1). The Aoudia *et al.* (2000) slip distribution on the rupture area is utilized as input for the pseudodynamic approach that estimates the peak slip velocity, the rupture velocity, and the rise-time distributions through the empirical relationships proposed by Guatteri *et al.* (2004). The velocity-structure model, specific for the studied area, is taken from Moratto *et al.* (2012).

The high-frequency stochastic computations take advantage of the parameters proposed by Malagnini *et al.* (2002), who studied wave propagation in northeastern Italy. In this study, local site effects are not accounted for; hence some discrepancies between the simulated ground motion and that experienced during the Friuli earthquake might be expected, in particular at the sites located on the Friuli plain. Figures 2 and 3 show a comparison of the time series and their relevant Fourier spectra, calculated and recorded at the stations of Tolmezzo and Codroipo, respectively.

It is worth noting that the synthetics are able to reproduce satisfactorily the main features of the, unfortunately, few observed data. In Codroipo, some differences can be observed in the east–west component and in the low-frequency part of the vertical component, which might be attributed to propagation effects not accounted for in the model. Furthermore, Figure S1 (available in the supplemental material to the article), depicting the synthetics for all of the analyzed sites, shows that the directivity and antidirectivity effects (in the northwest at southeast directions, respectively) play a crucial role in characterizing the strong motion, especially in near field. As expected, the strongest shaking is calculated to have occurred at Gemona, located above the rupture area, where the peak ground acceleration (PGA), the peak ground velocity (PGV) on the horizontal component, and the static offset in the vertical direction, are 553 cm/s^2, 47 cm/s, and 27 cm, respectively. Also in Tricesimo and Tolmezzo, very large values of ground shaking were determined (PGA = 181 and 216 cm/s^2, respectively).

Method

To simulate the real-time data analysis, we apply in playback, making use of the calculated synthetic seismograms, the procedure proposed in Parolai *et al.* (2015) for decentralized onsite early warning. In particular, the recordings are first low-pass filtered (corner frequency at 1 Hz) using a Gaussian filter, and to detect a possible event, a standard short-time average over long-time average algorithm in the time domain is applied. The data are then integrated in real time to velocity and displacement. The instantaneous peak ground displacement (Pd) in the vertical component during the first 3 s after the detection of an event is used to estimate the expected PGV in the horizontal component using the empirical relationship of Caruso *et al.* (2017). The PGVs are estimated for the mean and the 16% and the 84% confidence intervals, and these three values are continuously compared with the threshold values set in a traffic-light system based on the use of three matrices linking the expected ground motion to the possible damage (in seismic intensity; Parolai *et al.*, 2015). That is, although the analysis is carried out during the first 3 s after the event's detection, a red alarm, for example, can be issued well before the end of the 3 s window. In this study, the threshold levels linking the PGV to the possible damage (described through macroseismic intensities) are modified from those presented in Parolai *et al.* (2015), Parolai, Boxberger, *et al.* (2017), and Parolai, Oth, and Boxberger (2017) by considering the relationship of Worden *et al.* (2012). In the case at hand, a seismic intensity value of VI (related to a PGV of 6.7 cm/s) was used as the minimum threshold for the red status, corresponding to the very likely occurrence of slight structural damage. For further information about the procedure, the reader is referred to Parolai *et al.* (2015), Parolai, Boxberger, *et al.* (2017), and Parolai, Oth, and Boxberger (2017).

Results

The stations selected for the synthetic seismogram calculations are located within the areas that experienced macroseismic intensities (Medvedev–Sponheuer–Karnik scale) spanning from VI to X (Giorgetti, 1976). In the following, we show and discuss only some exemplary cases, with the remaining results presented in Figures S2–S14.

Figure 4 shows the vertical component of acceleration (top panel) and the modulus of the vector sum of the velocity in the horizontal plane for the Gemona site, which was located in the epicentral area and experienced a macroseismic intensity of X. As expected, because of the short epicentral distance (~9 km), although the earthquake was immediately detected, the shaking overstepped the threshold chosen before the alarm could be launched.

Figures 5 and 6 depict the results obtained for two sites (Cividale and Udine, Fig. 1) located nearly 25 km from the epicenter. In Cividale, the alarm is triggered 2.36 s after the event is detected, but the maximum ground motion observed on the horizontal component only reaches 4.88 cm/s, which is below the threshold of 6.7 cm/s. This is a case of an alarm followed by no consequences (*Enhanced alerts*, Parolai, Oth, and

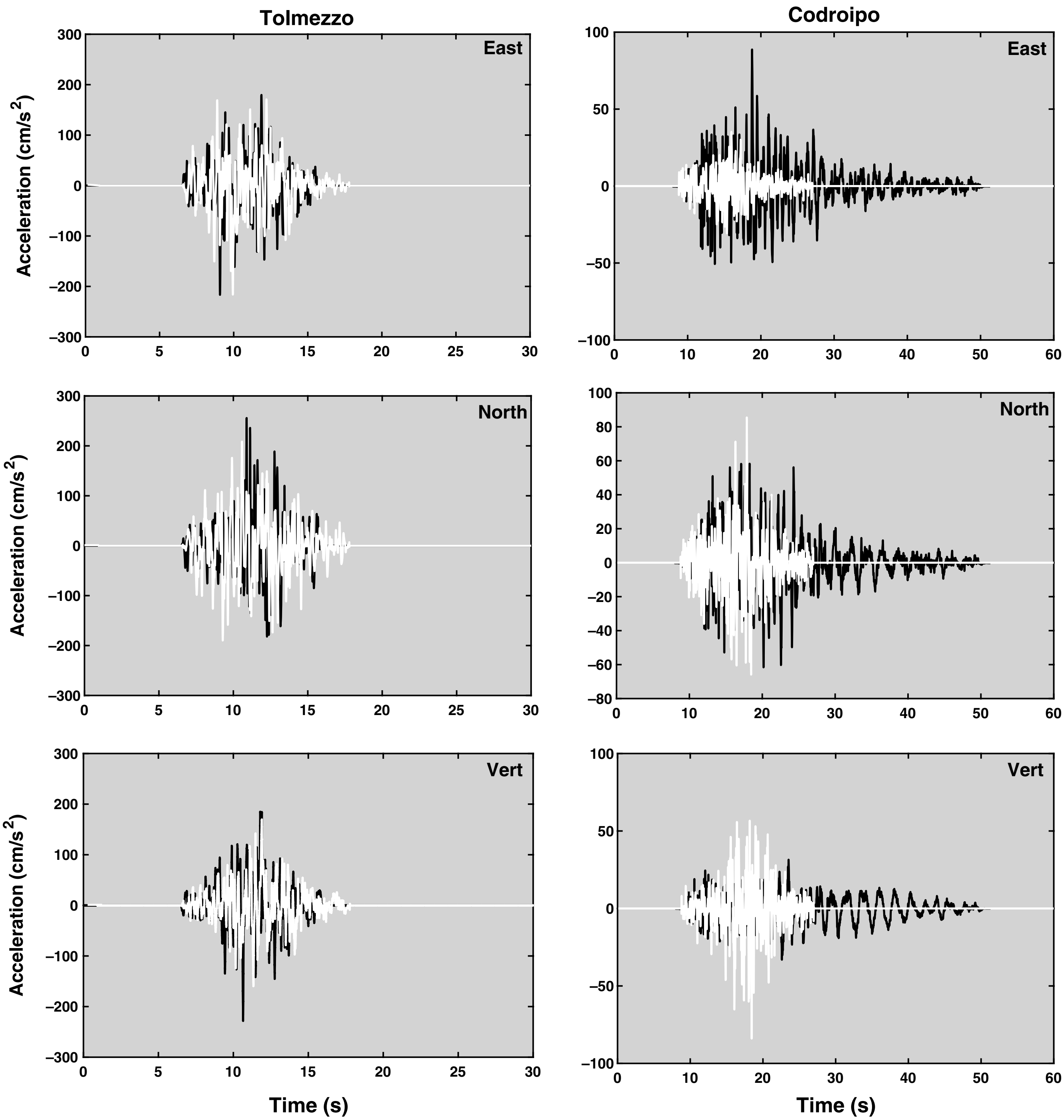

Figure 2. Recorded (black) and synthetic (white) seismograms for the 1976 Friuli earthquake in Tolmezzo and Codroipo (Fig. 1).

Boxberger, 2017), but with a level of shaking felt by the population (intensity V) that should not affect their trust in the system. It is worth noting that the observed macroseismic intensity in Cividale was VII, meaning that either some effects were not fully captured by the numerical simulations or/and it has a particularly vulnerable building stock and that, in any case, the alarm would have provided a lead time of 3.67 s before the arrival of the maximum shaking (which would not necessarily correspond to the *S*-wave arrival, see e.g., Caruso *et al.*, 2017; Parolai, Oth, and Boxberger, 2017).

In Udine, despite the similar epicentral distance, the seismograms appear to be shorter and with larger ground-motion amplitudes. The alarm is launched 0.68 s after the trigger and provides a lead time of 4.30 s before the 6.7 cm/s threshold is overstepped. The difference in the lead time is related not only to the finiteness of the fault (Zollo *et al.*, 2009) but also, as

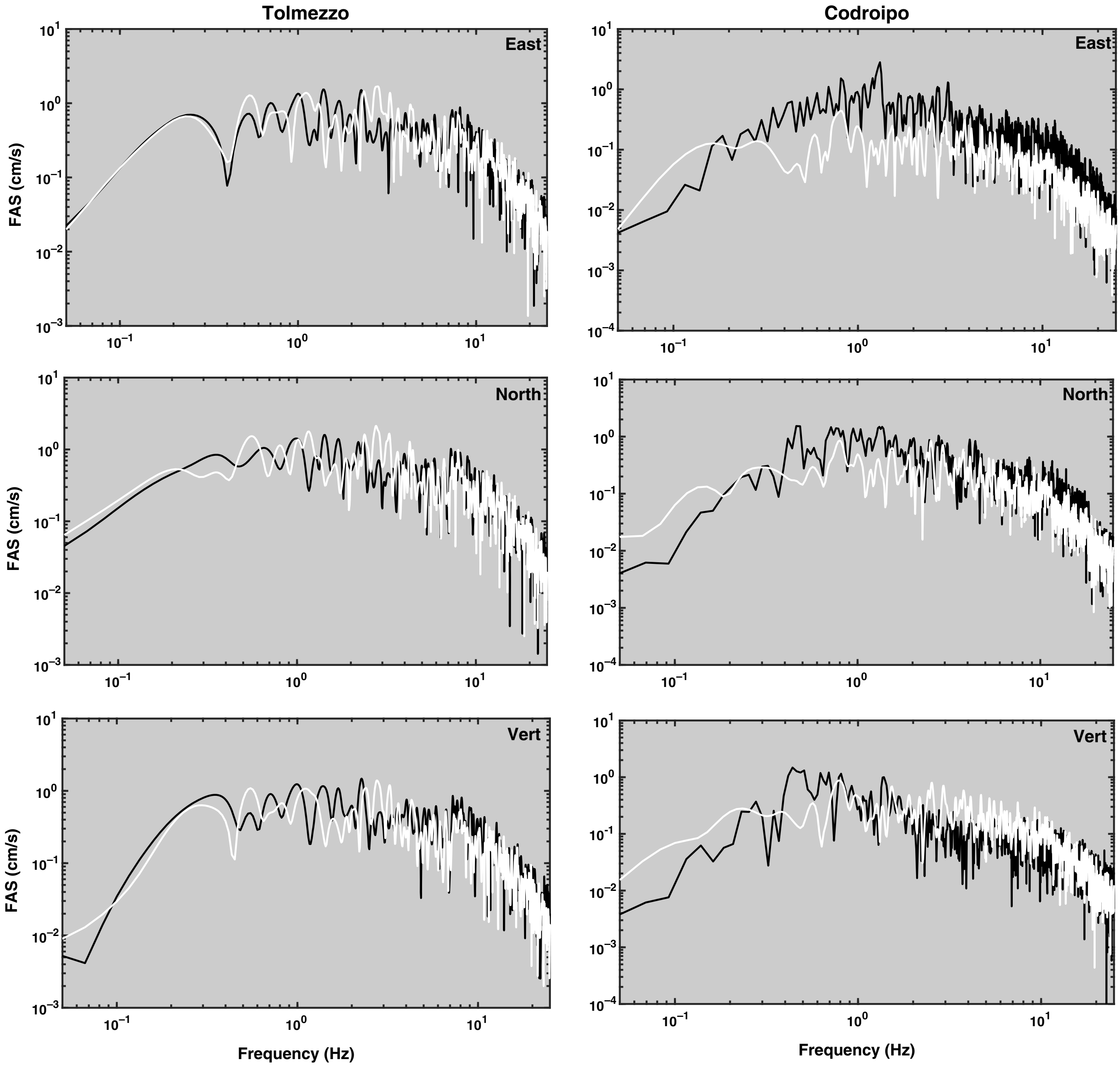

Figure 3. Fourier spectra of the recorded (black) and synthetic (white) seismograms of the 1976 Friuli earthquake in Tolmezzo and Codroipo (Fig. 1). FAS, Fourier amplitude spectrum.

shown by the different forms of the seismograms, to the source radiation and the slip distribution.

A similar behavior can be observed when comparing the stations of Spilimbergo and Tarvisio located at 34 and 35 km epicentral distance, respectively (Figs. S9 and S10).

Figures 7 and 8 show the results for the Cordenons and Forni di Sopra stations, located 54 km from the epicenter. At both stations, the alarm is raised nearly immediately after the trigger, but, despite the similar epicentral distances, the level of shaking (20 cm/s in Cordenons and 30 cm/s in Forni di Sopra) and the lead times (6.18 s in Cordenons and 8.85 s in Forni di Sopra) are quite different.

In summary, the applied procedure declared a red alarm (expected overstep of the 6.7 cm/s threshold) at all of the stations except Trieste (Fig. 1). In Trieste, a green status was declared, although for a short time (0.1 s) the 3.1 cm/s threshold was overstepped. This, following Parolai, Oth, and Boxberger (2017), could be defined as a *Missed Alert* (shaking felt by the population [intensity V] that would not lead to serious consequences). In 13 out of 17 cases, the red alarm correctly forecasted that the 6.7 cm/s threshold would have been overstepped. In the remaining four cases, the level of shaking was overpredicted, but the simulated values ranged

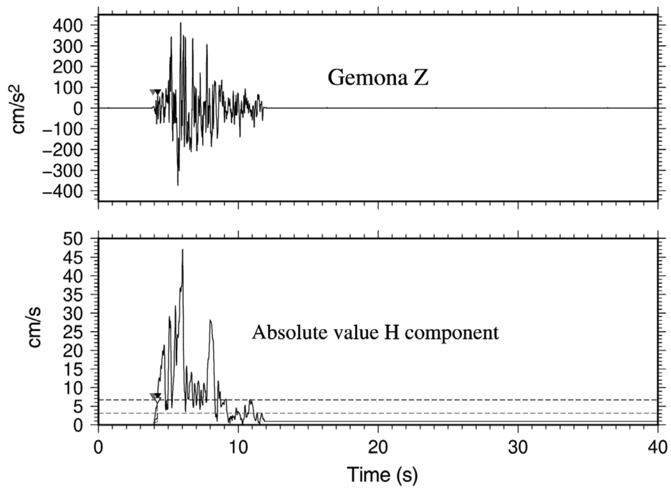

Figure 4. (Top) The vertical-component acceleration. The gray inverted triangle indicates the trigger time. The black inverted triangle indicates the alarm time. (Bottom) The vector sum of the velocity in the horizontal plane. The gray dashed line indicates the 3.1 cm/s threshold (intensity V); the dark gray dashed line indicates the 6.7 cm/s threshold. Gray and black inverted triangles are the same as in the top panel. The inverted gray triangle indicates the time when the 6.7 cm/s threshold is reached.

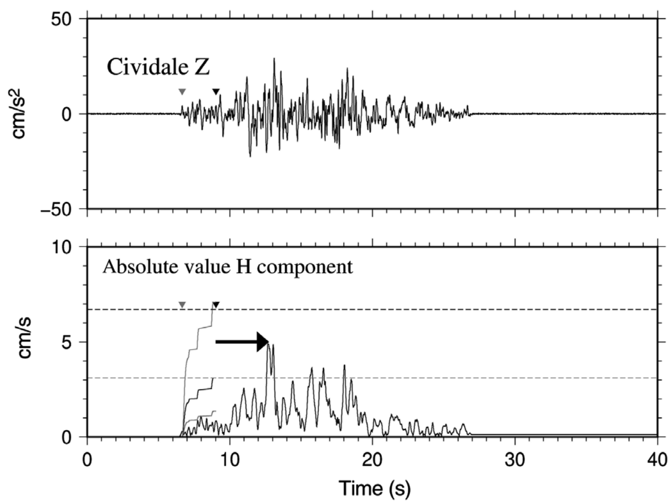

Figure 5. The same as for Figure 4, but for Cividale. Note in the bottom panel the predicted peak ground velocity (PGV) values (84% and 16% confidence intervals in gray and the mean in black) are estimated from the vertical component. The arrow indicates the lead time.

between 4.1 (Gorizia) and 6.3 cm/s (Palmanova). As indicated before, these *Enhanced alerts* are relevant to a level of shaking felt by the population (intensity V). In general, at all of the localities except Trieste, Gemona (lead time −0.01 s), and Tolmezzo (0.32 s) information about potentially dangerous shaking could have reached the population in the considered sites.

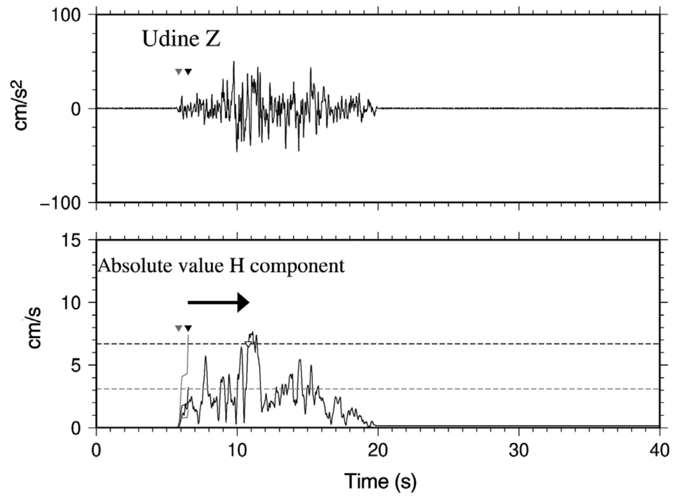

Figure 6. The same as for Figure 4, but for Udine. Note in the bottom panel the predicted PGV values (84% and 16% confidence intervals in gray and the mean in black) are estimated from the vertical component. The arrow indicates the lead time.

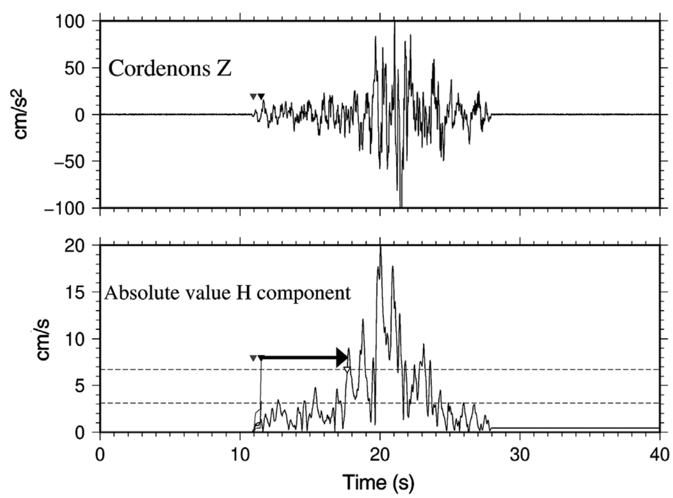

Figure 7. The same as for Figure 4, but for Cordenons. Note in the bottom panel the predicted PGV values (84% and 16% confidence intervals in gray and the mean in black) estimated from the vertical component. The arrow indicates the lead time.

In particular, we notice that lead times ranging from 2.8 (Tricesimo, observed macroseismic intensity VII–VIII) to 8.85 s (Forni di Sopra, observed macroseismic intensity VII–VIII) could have been available in urbanized areas, where structural damage to buildings and infrastructures can be expected in cases of future seismic events. This amount of time could have helped in improving the response of the population, mitigating the effects (at least in terms of injured people) of the earthquake.

Figure 9 shows the lead time versus station back-azimuth and epicentral distance. In the case of enhanced or missed

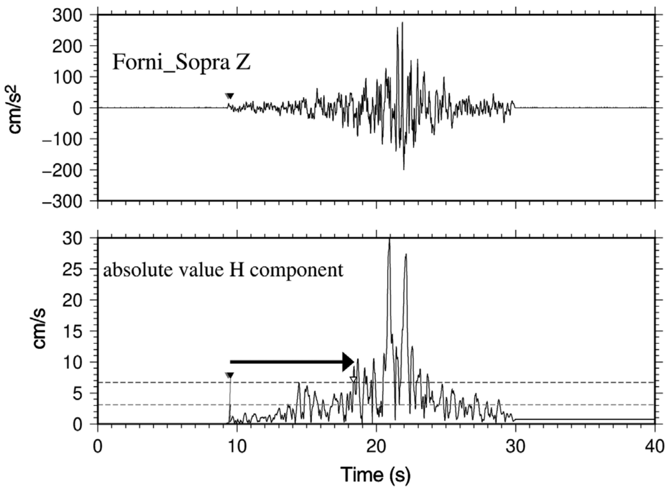

Figure 8. The same as for Figure 4, but for Forni di Sopra. Note in the bottom panel the predicted PGV values (84% and 16% confidence intervals in gray and the mean in black) estimated from the vertical component. The arrow indicates the lead time.

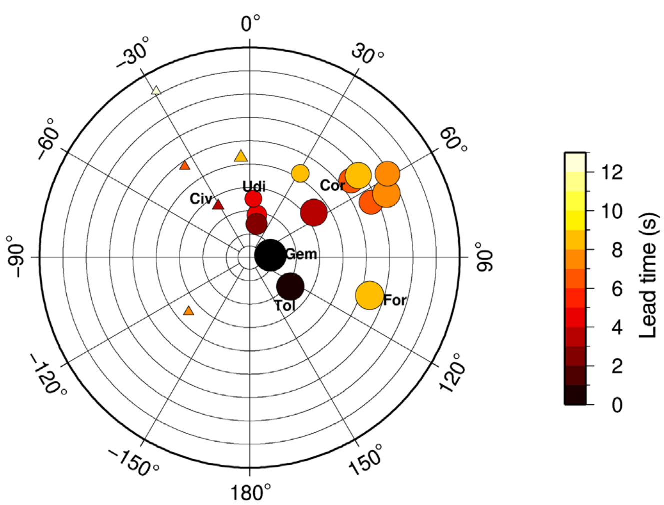

Figure 9. Lead time versus station back azimuth. The radius length is 90 km. The symbol size is proportional to the maximum horizontal ground motion. Triangles indicate stations with *Missed* or *Enhanced Alerts*. Circles are stations with *Alarm*. Civ, Cividale; Cor, Cordenons; For, Forni di Sopra; Gem, Gemona; Tol, Tolmezzo; Udi, Udine. The color version of this figure is available only in the electronic edition.

alerts (triangles in Fig. 9), the lead time was approximated by the time from the alarm or trigger to the observed maximum of the horizontal component on the simulated seismograms. The size of the symbols is proportional to the observed velocity maximum of the horizontal component. A clear source directivity effect is shown by the azimuthal dependence of the ground-motion amplitude. However, a clear lead-time back-azimuth dependence can also be observed (for similar epicentral

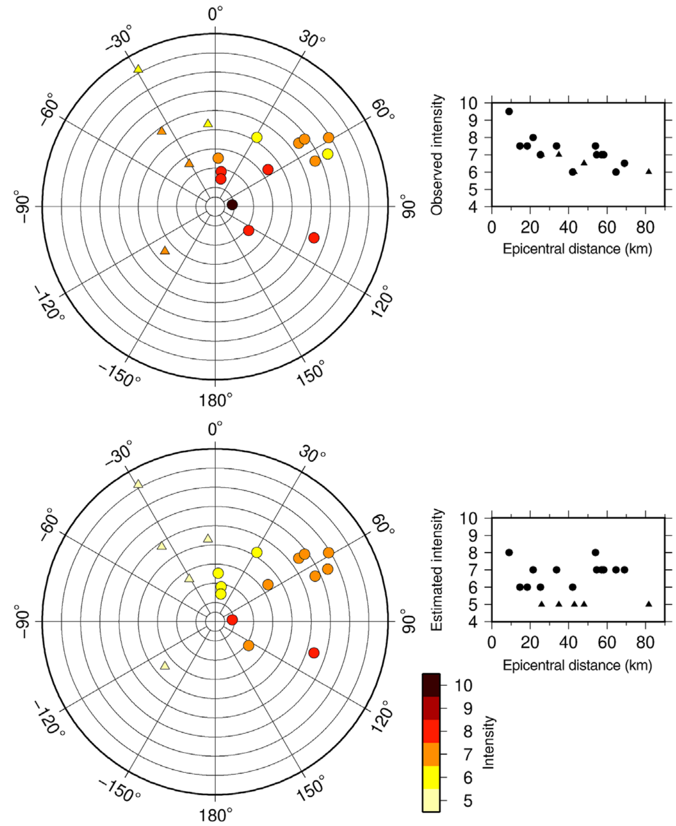

Figure 10. (Top) Observed macroseismic intensities versus back azimuth (left) and epicentral distance (right). (Bottom) Calculated macroseismic intensities versus back azimuth (left) and epicentral distance (right). Triangles indicate stations with *Missed* or *Enhanced Alerts*. Circles are stations with *Alarm*. The color version of this figure is available only in the electronic edition.

distances), in particular for Cordenons and Forni di Sopra but also (see Fig. 1) for Udine and Tolmezzo, where less than 7 km epicentral distance difference cannot alone explain the estimated 4 s difference in the lead times.

Finally, we estimated macroseismic intensities at each considered site using the Worden *et al.* (2012) relationships for the PGV and compared them with the observed values (Fig. 10). The observed macroseismic intensities are represented using half of a degree in case they had been assigned as, for example, VII–VIII, whereas the estimated ones are depicted using the nearest integer to the value. This might explain some of the differences between the observed and the calculated macroseismic intensities. Some other factors responsible for the discrepancies are listed as follows:

- the harmonization and smoothing of the observed intensity field, likely done at the time of the survey after the earthquake;
- the missing contribution of site effects (especially for sites located in the northeast back-azimuth quadrant) to the synthetic seismograms;

- the approximation done when converting ground-motion values to intensities (which are not accounting for the local building stock vulnerability and the spatial significance of macroseismic intensities); and
- the choice of using the Worden *et al.* (2012) relationships that might underestimate the level of damage for the building stock existing in northeastern Italy in 1976 (although it might be more appropriate for the stock existing now).

Despite these absolute differences (we remark that the synthetics lead in general to lower macroseismic intensities than that observed), the azimuthal trend of variability of the intensities is satisfactory.

Discussion

The results obtained in this study show that the adoption of a DOSEEW, in the case of the repetition of an event like the 1976 M_s 6.5 Friuli earthquake, might provide several seconds of lead time at the investigated sites that are representative of localities affected by macroseismic intensities larger than VI. A quantitative estimation of the benefit derived by an EEW system is always difficult (Strauss and Allen, 2016; Woo *et al.*, 2016). In our case, because most of the casualties happened in the blind zone (with macroseismic intensity ≥ VIII), we speculated on the mitigation effect that an alarm could have had on the number of injured persons in the areas where a macroseismic intensity between VI and VII–VIII was assigned.

To do this, we estimated the number of injured persons within the areas affected by the same level of macroseismic intensities. The damage reports collected after the 1976 mainshock (Di Sopra, 1976) contained the occupants of damaged buildings for each damaged area and municipality, whereas the number of substantially injured people (i.e., that needed to be hospitalized) was available only for homogeneously damaged areas (specifically defined by Di Sopra, 1976). Thus, we disaggregated the total number of injured people at the municipality scale, assuming a constant proportion between injured people and occupants of damaged buildings in these areas. Finally, we aggregated the number of injured people based on the macroseismic intensity classification of each municipality (Giorgetti, 1976).

We estimated that in the areas that experience a macroseismic intensity of VI–VII, VII, VII–VIII, and VIII, the number of injured persons were 10, 113, 100, and 457, respectively. The results obtained for the investigated municipalities are shown in Table 1. For example, in Cividale, where the observed intensity was assigned to VII and the lead time was estimated to be 3.67 s, 18 persons were estimated to have been injured. Although short, this lead time could have helped to mitigate against the effects of the event. In Cordenons (intensity VII), the estimated 6.19 s of lead time could have helped reduce the estimated number of five injured. A similar number of persons who were injured in Tarvisio (VII) could have taken advantage of a lead time of 7.33 s. In Pordenone (intensity VII), the estimated 27 injured people could have benefited from the estimated 8.34 s lead time to undertake appropriate actions. In Udine (VII), 4.3 s of lead time could have helped in mitigating the estimated number of 53 injured. In Forni di Sopra (intensity VII–VIII), 8.85 s of lead time would have been available for the four estimated injured persons. In Sacile (intensity VI–VII), the six estimated injured could have benefited from 7.84 s of lead time, and in Spilimbergo and Tavagnacco (VII–VIII), a lead time of 3.63 and 4.29 s could have been available for the estimated 24 and 10 injured, respectively. In Tricesimo (VII–VIII), the lead time would have been very short (2.83 s), allowing only very rapid actions, if well trained, for the estimated 10 injured.

TABLE 1
Summary of the Localities and Lead Times versus Injured Person during the 1976 Friuli Earthquake

Locality	Lead Time (s)	1976 Intensity	1976 Injured
Cividale	3.67	VII	18
Cordenons	6.19	VII	5
Tarvisio	7.33	VII	5
Pordenone	8.34	VII	27
Udine	4.30	VII	53
Forni di Sopra	8.85	VII–VIII	4
Sacile	7.84	VI–VII	6
Tavagnacco	4.29	VII–VIII	24
Spilimbergo	3.63	VII–VIII	10
Tricesimo	2.83	VII–VIII	10

Altogether, if all of the inhabitants could have been reached by an alarm and if their reactions had been appropriate, then the availability of an early warning to the population in all of the municipalities affected by macroseismic intensity VI to VII–VIII (with an estimated number of injured equal to 223) might have helped in reducing the number of injured persons (total number of nearly 2000) by more than 10%. This is due to the magnitude of the event resulting in a large concentration of fatalities and injured mainly within a restricted area around the epicenter. A prompt early warning in cases of larger magnitude events, which would result in a wider area of structural destruction and damage, could significantly reduce the absolute number of injured persons. The casualty estimation presented here is based on reasonable assumptions: relationship between injured people and collapsed buildings have been postulated by Coburn and Spence (2002) and confirmed by subsequent empirical studies (Ellidokuz *et al.*, 2005; So and Spence, 2013; Pan *et al.*, 2019). However, its validity is limited by the small amount of available data and the complexity of local factors that complicate injury patterns (e.g., people's behavior and evasive action, see e.g., So and Spence, 2013). In particular, after the 1976 Friuli earthquake, no data were collected on minor and moderate injuries that did not require hospitalization, but we speculate that their number also may be reduced by prompt early warning systems. Such benefits should be strongly related to the efficacy of communication and education strategies, the degree of participation of the involved communities, and the definition of effective decision-making protocols (Garcia and Fearnley, 2012).

Considering the importance of the industrial facilities in the area and the impact that their rapid restoration to normal working conditions has for mitigating indirect losses, we investigated the possible impact of an automatic early warning action for two main industrial plants in the region. The first one is the Trans-Alpine (TAL) pipeline, which crosses the region (approximately in the direction of Trieste, Udine, Tolmezzo, and then to the north toward Austria, Fig. 1) and has several pumping stations in the region. The pipeline provides crude oil necessary for satisfying 40% of the energy needs of Germany and the Czech Republic and 90% of that for Austria. For this pipeline, the possibility of allowing an early interruption of its use during the event would potentially minimize the possibility of leakage in case of rupture (that did not happen during the 1976 events). If rupture happens, a postevent stoppage of the system would certainly generate greater losses (M. Szalay and M. Diminich, personal comm., 2020). Hence, depending on the location of the next disastrous earthquake in the region, several seconds of lead time could be available for a large portion of the pipeline to allow emergency (and probably automatic) actions to be taken.

In the case of a repetition of the 1976 event (which generated displacements of the pipeline by up to 10 cm), the lead time ranges from more than 4 to nearly 8 s in the areas with soft sedimentary material between Udine and Tavagnacco. Nowadays, the pumping system is stopped only after a certain threshold of shaking (0.6 cm/s lasting 1 s, as calculated by integrating the data of an accelerometer with transducer) is overstepped (M. Diminich, personal comm., 2020). This system is not intended for earthquakes, but to stop engines to protect the casing and pipeline in the case of damages on the pumps impellers. We simulated the application of this threshold system on all of the synthetic seismograms that we calculated, under the assumption that the existing installed sensors are not filtering the data. We found that the threshold system would have systematically stopped the pumping after the DOSEEW system issued an alert (from less than 1 s to several seconds, such as in Forni di Sopra and Gorizia). In particular, the alarm would have been issued 0.46, 0.7, and 1.6 s later in Tolmezzo, Udine, and Tavagnacco, respectively. It is worth noting that for Trieste, although the DOSEEW system would have sent a warning, but, correctly, would not have triggered any automatic actions (green status) due to the small dynamic displacement (of the order of 1 cm in the vertical component), the threshold system would have triggered automatic action 12.64 s after the DOSEEW information. Considering that the sensors actually used by the company, being focused on the performance of a specific component of the infrastructure, apply high-pass filtering to the data (10 Hz corner frequency), most of the energy in the seismogram would be lost. The test that we made showed that, even in Gemona, the threshold system would not have triggered the alarm.

In general, a threshold-based system requires fixing the threshold value either at a relatively low level of shaking (therefore stopping the plant, even if later, larger and more dangerous levels of motion will not be exceeded by the same event) or at large values, taking actions only during the large shaking phase. For this reason, a few sensors running the OSEEW system have been recently installed along the pipeline to evaluate their performance for their possible operational usage in the future.

Furthermore, we investigated the possible benefit that an early warning might have on the assembly line of a large facility (>1100 employees) producing electronic components of LED lights operating in the Tolmezzo industrial site. In the case of the repetition of the 1976 event, the plant would lie at the border of the blind zone, therefore with no advantage from an early warning. An early warning could be useful in the case in which a similar magnitude event occurs in one of the other seismogenic areas in the region (Slejko, 2018) for which automated actions that are not existent now (R. Argentin, personal comm., 2020) could be planned. However, if the onsite system would also include the possibility of monitoring the factory assembly line and building and could also work during the aftershock sequence (Bindi *et al.*, 2016) it could help improve the rapid-risk mitigation actions and therefore enhance the workers' safety. To this regard, a DOSEEW system with the capability of triggering automatic actions is currently being installed in the factory.

Conclusions

In this study, we estimated the potential benefits that an DOSEEW system, based on recently installed strong-motion sensors, could provide in the case of the repetition of the 1976 Friuli earthquake. Although the advantages of having a dense strong-motion network are obvious when considering the need for a robust and accurate rapid damage assessment that can improve the response to a damaging seismic event, its contribution to seismic risk mitigation through the adoption of an EEW system might not be certain. This study, based on a single scenario, shows that the lead time in the case of the 1976 events, with the actual station deployment, could have been sufficient for a large part of the affected area to mitigate at least the number of injured persons. Interestingly, the application of the OSEEW approach to the synthetic seismograms showed a strong dependence of the lead time not only on the finite dimension of the fault but also on the slip distribution. Because of the size of the event, most of the casualties occurred within what is defined as the blind zone; however, a significant number of injured persons could have benefited, if appropriately trained, from the alarm coming from an early warning system. We estimated that a reduction of 10% of injured persons could be achieved. Although not large, this could have certainly helped in mitigating, with other preparation and rapid response measures, the impact of the event.

These results, although specific for the 1976 Friuli earthquake scenario, can easily be extended and adapted for the other possible seismogenic sources existing in the region.

Finally, following the Friuli saying relevant to reconstruction after the 1976 earthquake "First the factories, then the houses, and then the churches," we also tried to investigate the potential effect of an early warning system for two industrial facilities.

We found that the TAL pipeline could benefit from several seconds of lead time, allowing automatic procedures for the stoppage of the plant, therefore mitigating the risk of the pipeline's damage and subsequent oil leakage. On the other hand, the factories operating in Tolmezzo would lie within the blind zone in the case of a repetition of the 1976 Friuli earthquake. However, in the case of other earthquake scenarios in the region, the factories could benefit from an alarm with several seconds of lead time that would allow automated actions to be employed, hence potentially improving the workers' safety.

Further studies and testing of the systems are necessary for better evaluating the cost benefit analysis of an EEW system in the region. In particular, the two installations along the TAL and in the factory in Tolmezzo that are currently being deployed will provide useful data for this evaluation.

Data and Resources

No recorded data were used for the analysis in this article. The strong-motion data of Figures 2 and 3 are available from Italian Accelerometric Archive v.3.0 (doi: 10.13127/itaca.3.0; Luzi *et al.*, 2019). The synthetic seismograms are available from the authors upon request. The other relevant data are from Progetto Edifici Sentinella, supported by the Regional Civil Protection of Friuli Venezia Giulia, and the Interreg Armonia Project (https://www.inogs.it/en/content/armonia-rete-di-monitoraggio-accelerometrico-tempo-reale-di-siti-ed-edifici-italia-ed, last accessed July 2020). Supplemental material for this article includes a figure showing all three-component synthetic seismograms calculated at the considered stations (Fig. S1) and Figures S2–S14, which show the results of the analysis for the analyzed stations not included in the article.

Acknowledgments

The authors thank Editor-in-Chief A. Bent, A. Oth, and an anonymous reviewer for the positive and constructive comments and suggestions that helped in improving the article. The authors thank Massimo Diminich and Mauro Szalay (Trans-Alpine [TAL] Group) and Renzo Argentin (Automotive Lighting SpA) for useful discussions. The authors thank F. Marino (Museo Tiere Motus Venzone) and the staff of the Library "Livio Paladin" (Palazzo della Regione Trieste) for providing information about the number of injured persons. The figures were drawn using the Generic Mapping Tool (Wessel and Smith, 1991). K. Fleming kindly improved our English.

References

Allen, R. M., P. Gasparini, O. Kamigaichi, and M. Böse (2009). The status of earthquake early warning around the world: an introductory overview, *Seismol. Res. Lett.* **80,** 682–693, doi: 10.1785/gssrl.80.5.682.

Aoudia, A., A. Saraò, B. Bukchin, and P. Suhadolc (2000). The 1976 Friuli (NE Italy) thrust faulting earthquake: A reappraisal 23 years later, *Geophys. Res. Lett.* **27,** 577–580.

Bindi, D., I. Iervolino, and S. Parolai (2016). On-site structure-specific real-time risk assessment: Perspectives from the REAKT project, *Bull. Earthq. Eng.* **14,** no. 9, 2471–2493, doi: 10.1007/s10518-016-9889-4.

Boore, D. M. (2009). Comparing stochastic point-source and finite-source ground motion simulations: SMSIM and EXSIM, *Bull. Seismol. Soc. Am.* **99,** 3202–3216.

Caruso, A., S. Colombelli, L. Elia, M. Picozzi, and A. Zollo (2017). An on-site alert level early warning system for Italy, *J. Geophys. Res.* **122,** 2106–2118, doi: 10.1002/2016JB013403.

Clinton, J., A. Zollo, A. Marmureanu, C. Zulfikar, and S. Parolai (2016). State-of-the art and future of earthquake early warning in the European region, *Bull. Earthq. Eng.* **14,** no. 9, 2441–2458.

Coburn, A. W., and R. J. S. Spence (2002). *Earthquake Protection*, John Wiley & Sons, Ltd, first published September 2002, 436 pp., Print ISBN: 9780471496144, Online ISBN: 9780470855188, doi: 10.1002/0470855185.

Di Sopra, L. (1976). *Stima dei danni sisma 6 maggio 1976*, Regione Autonoma Friuli Venezia-Giulia, Segreteria Generale Straordinaria, Udine, 1976, Library 'Livio Paladin', Palazzo della Regione, Trieste, Italy (in Italian).

Ellidokuz, H., R. Ucku, U. Y. Aydin, and E. Ellidokuz (2005). Risk factors for death and injuries in earthquake: cross-sectional study from Afyon, Turkey, *Croat. Med. J.* **46,** no. 4, 613–618.

Garcia, C., and C. J. Fearnley (2012). Evaluating critical links in early warning systems for natural hazards, *Environ. Hazards* **11,** no. 2, 123–137, doi: 10.1080/17477891.2011.609877.

Giorgetti, F. (1976). Isoseismal map of the May 6, 1976 Friuli earthquake, *Boll. Geofis. Teor. Appl.* **18,** 707–714.

Guatteri, M., P. M. Mai, and G. C. Beroza (2004). A pseudo-dynamic approximation to dynamic rupture models for strong ground motion prediction, *Bull. Seismol. Soc. Am.* **94,** 2051–2063.

Luzi, L., F. Pacor, and R. Puglia (2019). *Italian Accelerometric Archive v3.0*, Istituto Nazionale di Geofisica e Vulcanologia, Dipartimento della Protezione Civile Nazionale, doi: 10.13127/itaca.3.0.

Malagnini, L., A. Akinci, R. B. Herrmann, N. A. Pino, and L. Scognamiglio (2002). Characteristics of the ground motion in Northeastern Italy, *Bull. Seismol. Soc. Am.* **92,** 2186–2204.

Moratto, L., P. Suhadolc, and G. Costa (2012). Finite-fault parameters of the September 1976 $M > 5$ aftershocks in Friuli (NE Italy), *Tectonophysics* **536/537,** 44–60.

Moratto, L., A. Vuan, and A. Saraò (2015). A hybrid approach for broadband simulations of strong ground motion: the case of the 2008 Iwate–Miyagi Nairiku earthquake, *Bull. Seismol. Soc. Am.* **105,** 2823–2829.

Motazedian, D., and G. M. Atkinson (2005). Stochastic finite-fault modeling based on a dynamic corner frequency, *Bull. Seismol. Soc. Am.* **95,** 995–1010.

Pan, S. T., Y. Y. Cheng, C. L. Wu, R. H. Chang, C. Chiu, N. P. Foo, P. T. Chen, T. Y. Wang, L. H. Chen, C. J. Chen, *et al.* (2019). Association of injury pattern and entrapment location inside damaged buildings in the 2016 Taiwan earthquake, *J. Formos. Med. Assoc.* **118,** 311–323, doi: 10.1016/j.jfma.2018.05.012.

Parolai, S., D. Bindi, T. Boxberger, C. Milkereit, K. Fleming, and M. Pittore (2015). On-site early warning and rapid damage forecasting using single stations: Outcomes from the REAKT project, *Seismol. Res. Lett.* **86,** no. 5, 1393–1404, doi: 10.1785/0220140205.

Parolai, S., T. Boxberger, M. Pilz, K. Fleming, M. Haas, M. Pittore, B. Petrovic, B. Moldobekov, A. Zubovich, and J. Lauterjung (2017). Assessing earthquake early warning using sparse networks in developing countries: Case study of the Kyrgyz Republic, *Front. Earth Sci.* **5,** 74, doi: 10.3389/feart.2017.00074.

Parolai, S., A. Oth, and T. Boxberger (2017). Performance of GFZ decentralized on site earthquake early warning software (GFZ-Sentry): Application to K-NET and KIK-net recordings (Japan), *Seismol. Res. Lett.* **88,** no. 6, 1480–1490, doi: 10.1785/0220170048.

Pesaresi, D., M. Picozzi, M. Živčić, W. Lenhardt, M. Mucciarelli, L. Elia, A. Zollo, and A. Gosar (2017). A cross-border regional earthquake early warning system: PRESTo@CE3RN, *Nat. Hazards* **86,** 431–440, doi: 10.1007/s11069-016-2695-0.

Picozzi, M., L. Elia, D. Pesaresi, A. Zollo, M. Mucciarelli, A. Gosar, W. Lenhardt, and M. Živčić (2015). Transnational earthquake early warning (EEW) in Northeastern Italy, Slovenia and Austria: First experience with PRESTo at the CE3R Network, *Adv. Geosci.* **40,** 51–61, doi: 10.5194/adgeo-40-51-2015.

Rebez, A., I. Cecić, G. Renner, D. Sandron, and D. Slejko (2018). Misunderstood "forecasts": Two case histories from former Yugoslavia and Italy, *Boll. Geofis. Teor. Appl.* **59,** no. 4, 481–504, doi: 10.4430/bgta0244.

Rovida, A., M. Locati, R. Camassi, B. Lolli, and P. Gasperini (Editors) (2016). *CPTI15, the 2015 Version of the Parametric Catalogue of Italian Earthquakes*, Istituto Nazionale di Geofisica e Vulcanologia, doi: 10.6092/INGV.IT-CPTI15.

Slejko, D. (2018). What science remains of the 1976 Friuli earthquake? *Boll. Geofis. Teor. Appl.* **59,** no. 4, 327–350, doi: 10.4430/bgta0224.

So, E., and R. Spence (2013). Estimating shaking-induced casualties and building damage for global earthquake events: A proposed modelling approach, *Bull. Earthq. Eng.* **11,** 347–363, doi: 10.1007/s10518-012-9373-8.

Spudich, P., and L. Xu (2003). Documentation of software package Compsyn sxv3.11: Programs for earthquake ground motion calculation using complete 1-D Green's functions, in *International Handbook of Earthquake and Engineering Seismology*, CD, Int. Ass. Of Seismology and Physics of Earth's Interior, Academic Press, Cambridge, Massachusetts.

Strauss, J. A., and R. M. Allen (2016). Benefits and costs of earthquake early warning, *Seismol. Res. Lett.* **87,** no. 3, 765–772, doi: 10.1785/0220150149.

Wenzel, F., and J. Zschau (2014). *Early Warning for Geological Disasters: Scientific Methods and Current Practice*, Springer-Verlag, Berlin, Germany.

Wessel, P., and W. H. F. Smith (1991). Free software helps map and display data, *Eos Trans. AGU* **72,** 445–446.

Woo, G., M. Gobbato, and N. Shome (2016). The cost effectiveness of a West Coast earthquake early warning system, in *Earthquake and Induced Multi-Risk Early Warning and Rapid Response. Cahier du Centre Europeen de Geodynamique et de Seismologie*, A. Oth and S. Parolai (Editors), Vol. 31, 101–112.

Worden, C. B., M. C. Gerstenberger, D. A. Rhoades, and D. J. Wald (2012). Probabilistic relationships between ground-motion parameters and modified Mercalli intensity in California, *Bull. Seismol. Soc. Am.* **102,** no. 1, 204–221, doi: 10.1785/0120110156.

Wu, Y., W. Liang, H. Mittal, W. Chao, C. Lin, B. Huang, and C. Lin (2016). Performance of a low-cost earthquake early warning system (*P*-alert) during the 2016 M_L 6.4 Meinong (Taiwan) earthquake, *Seismol. Res. Lett.* **87,** no. 5, 1050–1059, doi: 10.1785/0220160058.

Zamberletti, G. (2018). Friuli 1976: Emergency management between the May and September earthquakes, *Boll. Geofis. Teor. Appl.* **59,** no. 4, 373–379, doi: 10.4430/bgta0213.

Zollo, A., G. Iannaccone, M. Lancieri, L. Cantore, V. Convertito, A. Emolo, G. Festa, F. Gallovič, M. Vassallo, C. Martino, *et al.* (2009). Earthquake early warning system in southern Italy: Methodologies and performance evaluation, *Geophys. Res. Lett.* **36,** L00B07, doi: 10.1029/2008GL036689.